Laser-spectroscopic study of Er doped $PbWO_4$ as laser and stimulated Raman scattering active crystals

Ilya Mirov[a], Vladimir V. Fedorov[b,*]

[a] University of Richmond, 28 Westhampton Way, Richmond, VA 23173 and Summer 2009 REU participant at the Department of Physics, University of Alabama at Birmingham;
[b] Center for Optical Sensors and Spectroscopies, Department of Physics, University of Alabama at Birmingham, 310 Campbell Hall, 1300 University Boulevard, Birmingham AL 35294, USA

ABSTRACT

PWO crystals were grown using the Czochralski method with concentrations from 0.2% to 4%. The polarized optical absorption, emission, and kinetics of fluorescence were measured at room temperature and low (14K) over a spectral range of 0.2 to 3 microns. The spectroscopic data were then used to calculate the absorption and luminescence cross sections. The maximum absorption cross at $^4I_{13/2} \rightarrow {}^4I_{15/2}$ transition section was calculated to be $\sigma=8.0x10^{-21}$ cm^2 at 1500 nm and E||z polarization of incident light. The measured luminescence lifetime at this transition was 5.6 ms.
Keywords: Er:$PbWO_4$, laser spectroscopy, Raman scattering active crystals.

1. Introduction

In recent years, stimulated Raman scattering (SRS) has become a well known technique for shifting the frequency of laser radiation to new spectral regions where direct laser oscillation is not available. The solid-state Raman lasers operating in the middle-infrared (mid-IR) spectral range are quite valuable for a variety of uses in medical, environmental, and sensing applications.

Lead tungstate $PbWO_4$(PWO) crystals have been known for decades for their scintillation properties [1]. They have garnered much interest since they have been selected as the material of choice for scintillation detectors used for the precise electromagnetic calorimeter (EMC) of the CMS experiment suited for the search of the Higgs boson in the intermediate mass region at the Large Hadron Collider (LHC) at CERN [2]. Because of all the accrued interest, a low-cost growth technique for large scale PWO crystals was developed. Later, interest in PWO crystals grew again because of their interesting properties as a nonlinear solid-state material for the SRS [3,4,5].

Additionally, the crystal structure of tungstate crystals allows the introduction of rare-earth (in this case Erbium) impurity ions and the utilization of these doped active crystals for lasing accompanied by Raman self conversion of radiation to a new spectral range [6].

The objective of this work is to study the spectroscopic characteristics of Er doped PWO crystals for identification of their feasibility as a combined self-gain Raman medium for the development of an effective fiber-bulk hybrid system operating at room temperature in the middle infrared spectral range.

2. $PbWO_4$ crystal properties

Some physical properties of tetragonal $PbWO_4$ single crystal are presented in Table 1. It is nonhygroscopic, low-cost, and features reasonable mechanical properties. As a scintillation material it has the lowest radiation length among other scintillators -- 0.85 cm. PWO is a negative uniaxial crystal with a wide range of optical transparency from 0.33 to 5.5 microns. The structure of PWO is depicted in Fig. 1 and is similar to Calcium Tungstate, or sheelite. In this structure, each Tungstate ion is surrounded by 4 oxygen ions and each lead ion is surrounded by 8 oxygen ions. As we know, the

* vfedorov@uab.edu; phone 1-205-934-5318; fax 1-205-934-8042

sheelite structure can accommodate many rare earth ions and Erbium in this crystal usually isomorphly substitutes lead which is accompanied by the formation of adjacent lead vacancy or an interstitial oxygen ion. Usually charge compensation is provided by a lead vacancy. As many crystals of sheelite structure, PWO has the strongest active Raman mode of 901 cm^{-1} provided by the vibrations of the Tungsten-oxygen tetrahedral.

Table 1. Some physical properties of $PbWO_4$ single crystals taken from references [3,4,5]

Necessity for moisture protection	no
Cost	low
Hardness (Mohs scale)	4–5
Melting point	1123 C
Density	8.28 g/cm^3
Radiation length, cm	0.85
Classification	Negative uniaxial
Unit cell	a= 5.462; c=12.049
Refractive Index at 700 nm	n_0=2.221±0.009; n_e=2.156±0.009
Optical transparency, μm	0.33-5.5
Strongest active Raman mode	901-905 cm^{-1}
Linewidth	4.7-4.3 cm^{-1} (RT)
1st Stokes Raman Gain coeff. & 1.06 μm, $cm \cdot GW^{-1}$	3.1

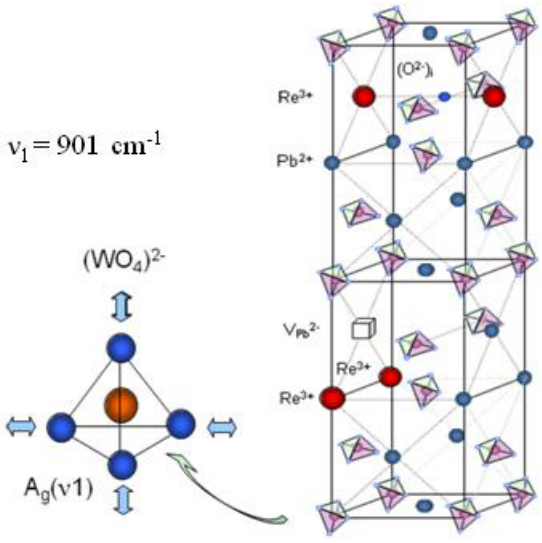

Fig. 1 The structure of $PbWO_4$ is similar to $CaWO_4$, (sheelite). Each W^{6+} is surrounded by four O^{2-} and each Pb^{2+} is surrounded by eight O^{2-} adopted [4]

3 Crystal Preparation and Experimental Techniques

The growth of the experimental crystals was done by the Czhochralski method in the inert atmosphere from the re-crystallized charge prepared from high purity chemicals. Six experimental crystals were grown with Erbium concentrations of 0.1%, 0.2%, 0.5%, 1%, 2% and 4% atomic percent. The crystals were all rectangular prisms of the size 5mm x 5mm x 10 mm, except the 2% and 4% concentrated crystals. They were sized 5mm x 5mm x 30mm and 5mm x 5mm x 40 mm, respectively. It should be noted that it was difficult to polish the crystals on the sides that were perpendicular to the optical axis. Due to the intrinsic properties of the crystals, these sides were much "softer" than the other sides of the crystals.

Room temperature (RT) absorption measurements in the visible and mid-IR spectral regions were performed with Shimadzu ''UV–VIS–NIR-3101PC" spectrophotometer. Unpolarized and polarized absorption spectra were also measured at low temperatures with a close-cycle helium cryostat (Janis Research Co, Inc., Model CCS-450) and a computer-controlled 0.75m Acton Research ''SpectraPro-750" spectrometer. The experimental set-up for measuring low-temperature absorption is depicted in Fig. 2. The kinetics of fluorescence and fluorescence spectra were measured using the Acton Research ARC-300 I spectrometer with photomultiplier, InGaAs, and InSb detectors. As an excitation source we used 532 nm radiation of second harmonic of CW Nd:YAG laser as well as 980 and 1532 nm radiations (5 ns pulse duration and 10 Hz repetition rate) of Spectra Physics optical parametric oscillator pumped by the 354 nm radiation of the third harmonic of QuantaRay Nd:YAG laser.

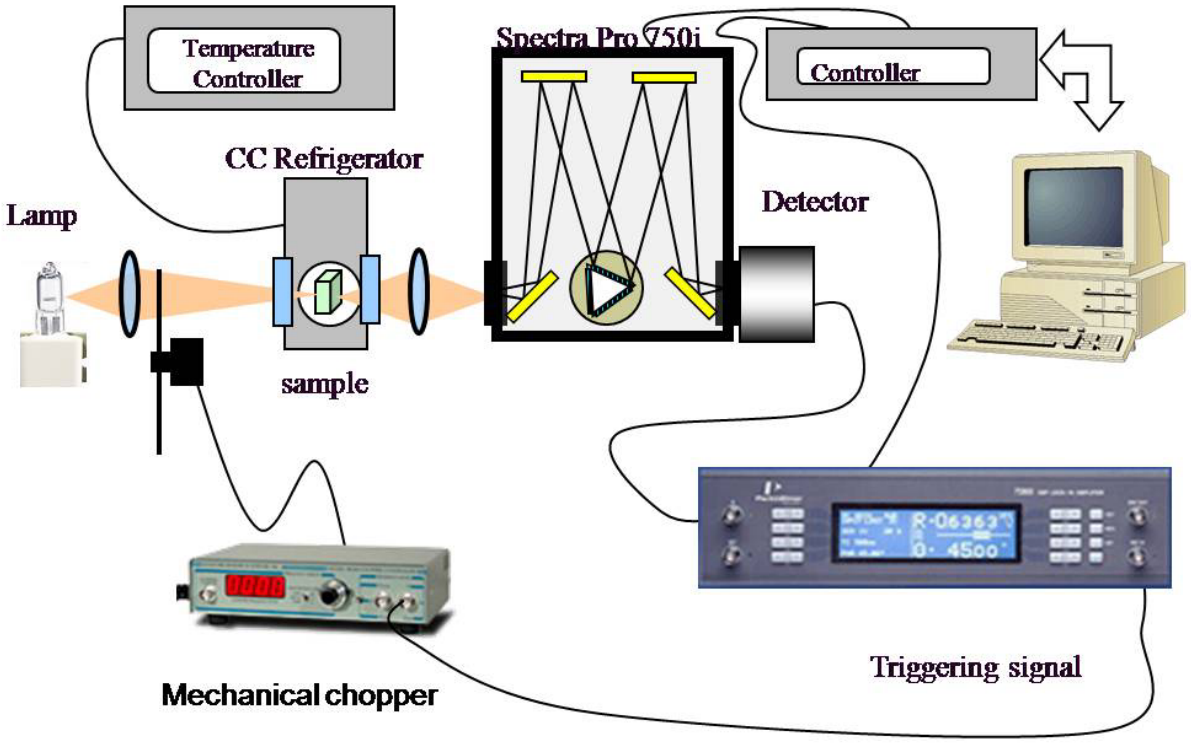

Fig. 2 Experimental Set-up for low temperature absorption measurements: Lamp (Acton Research TDS-429); Mechanical Chopper (Stanford Research Systems SR540); Temperature Controller (LakeShore Autotuning 330); Spectrometer (Spectra Pro 750i); Controller (Acton Research Corporation); Detectors (Acton Research Photomultiplier PD-439; Acton Research ID-441-C); CC Refrigerator: Helix Technology Corporation CTI-Cryogenics.

4 Spectroscopic Results and Discussion

Figure 3.A demonstrates unpolarized absorption spectra of 1% Er:PWO crystals in the UV-Visible spectral region. One can see that the fundamental UV absorption edge overlaps with Erbium ^{4}G multiplets near 350 nm transition from the ground state. One of the main uses for PWO in this work was the examination of its utilization as a gain material for the mid-IR spectral range. The RT absorption spectrum of undoped PWO crystal over the 2–10 μm range is depicted in Fig. 3B. As one can see from the graph, the PWO absorption spectrum begins from 4 μm and consists of several bands. Therefore the Er:PWO crystal, featuring effective optical phonon of ν= 901 cm^{-1}, is attractive active crystal for self-Raman lasing operating at 1.6 and 2.8 μm erbium transitions. It is interesting that even though the absorption of the crystal started from 3.9 μm, the crystal has a window of transparency, with a small loss, in the important IR spectral range of 4.5–4.9 μm.

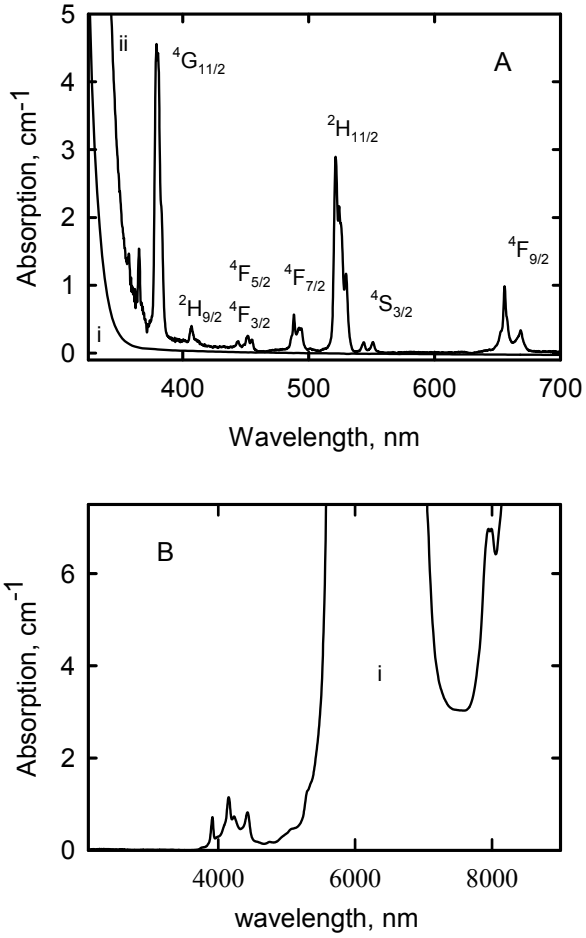

Fig.3 Unpolarized UV–visible (A) and mid-IR (B) absorption spectra of Er(4%):PWO (ii) and undoped PWO crystals (i)

Erbium multiplets of $PbWO_4$:Er located in the near IR spectral region are more interesting for laser application. The PWO crystals are uniaxial and two polarized spectra are necessary to characterize the electrical dipole transitions. However, as it was pointed out in [7], the considered transitions in Erbium are magnetic-dipole allowed and, therefore, three types of polarized spectra are necessary to characterize the optical properties: (a)E⊥z, H⊥z, k||z; (b) E⊥z, H||z, k⊥z;

(c) E||z, H||z, k⊥z. The results of the polarized measurements of the $^4I_{15/2}\rightarrow{}^4I_{9/2}$; $^4I_{15/2}\rightarrow{}^4I_{11/2}$; and $^4I_{15/2}\rightarrow{}^4I_{13/2}$ Er absorption at RT are depicted in Figs.4 A,B,C, respectively.

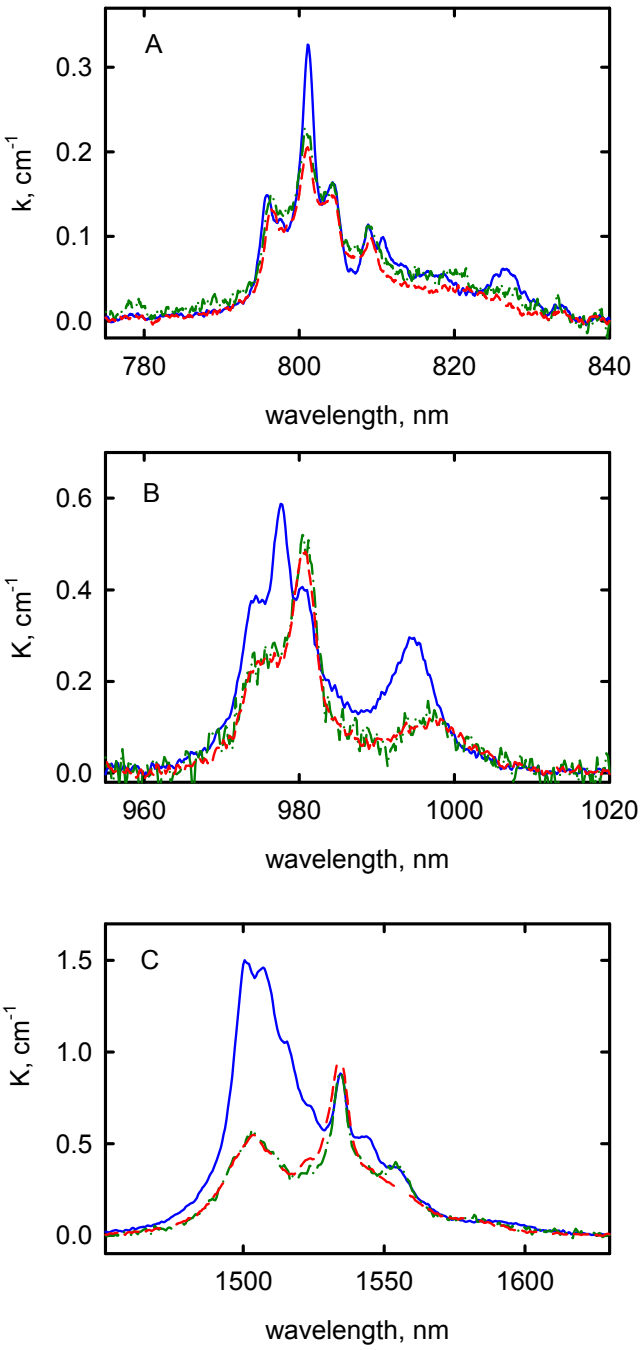

Fig. 4 **A:** Polarized absorption spectra $PbWO_4$:Er 2% crystal at $^4I_{15/2}\rightarrow{}^4I_{9/2}$ transition. Crystal Thickness: for E||Z = 0.485 cm (solid line), H||Z = 0.485 cm (dashed line), K||Z=0.272 cm (dash-dotted line). **B:** Polarized absorption spectra $PbWO_4$:Er 2% crystal at $^4I_{15/2}\rightarrow{}^4I_{11/2}$ transition. Crystal Thickness: for E||Z = 0.485 cm, H||Z = 0.485 cm, K||Z=0.272 cm. **C:** Polarized absorption spectra $PbWO_4$:Er 2% crystal at $^4I_{15/2}\rightarrow{}^4I_{13/2}$ transition. **Notice** that the coincidence of the peaks for A and B are caused because the magnetic dipole transitions are forbidden for ΔJ>1. For C, since ΔJ=1, the magnetic dipole transition is allowed and the peaks do not coincide.

As one can see the largest coefficient of absorption corresponds to the electric field of excitation light propagating along the PWO crystal optical axis (red). The difference in the absorption in the cases (E||z) and (H||z and k||z) can be explained by the input of magnetic-dipole transitions. For $^4I_{15/2} \rightarrow {}^4I_{13/2}$ Er absorption transition in the case of incident radiation with E||z polarization (red), the peak absorption of Er is 6 times larger than in the cases of H||z and k||z. In addition, for this polarization their absorption peaks for both short wave and long wave regions of the spectra are less pronounced. Because of this, this polarization looks attractive from the point of view of the realization of Er lasing under resonance excitation of the $^4I_{15/2} \rightarrow {}^4I_{13/2}$ transition. Low temperature absorption measurements allowed us to calculate the Stark level splitting for several multiplets: ΔE ($^4I_{15/2}$) = 300 cm^{-1}, ΔE ($^4I_{9/2}$) = 215 cm^{-1}, ΔE ($^4S_{3/2}$) = 40 cm^{-1}, and ΔE ($^4F_{5/2}$) = 53 cm^{-1}.

The cross-section of absorption of Er ions in PWO at 1505 nm transition can be calculated as coefficient proportionality between the coefficient of absorption and Er concentration. For its calculation polarized absorption spectra (depicted in Fig. 5) of PWO crystals with different concentration of Er ions were measured for E || Z.

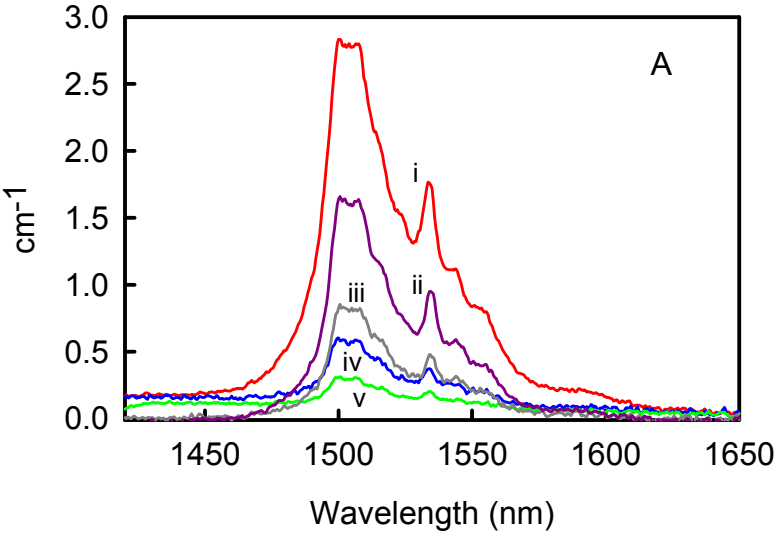

Fig. 5 Polarized absorption spectra of PWO crystals with different concentration of Er ions measured for E || Z. Crystal Thicknesses: 4% = 0.512 cm (i), 2% = 0.560 cm (ii), 1% = 0.331 cm (iii), 0.5% = 0.258 cm (iv), 0.2% = 0.484 cm (v).

The dependence of the peak absorption coefficient at 1505 nm as a function of the Er concentration is demonstrated in Fig. 6. As it can be seen from the figure, for low concentration of Er ions the dependence is linear, while for the high concentrations the peak absorption starts to roll-off from the linear dependence. Technological factors could be the most probable reasons for this behavior; in particular, it could be due to the saturation of Er doping of the PWO crystal with the increase of Er concentration in the melt.

The cross-section of absorption of Er ions was calculated with the use of the linear extrapolation of the coefficient of absorption for low concentrations of Er (see Fig. 6). The maximum absorption cross section was estimated to be $\sigma=8.0 \times 10^{-21}$ cm^2 at 1505 nm and E||z polarization of incident light.

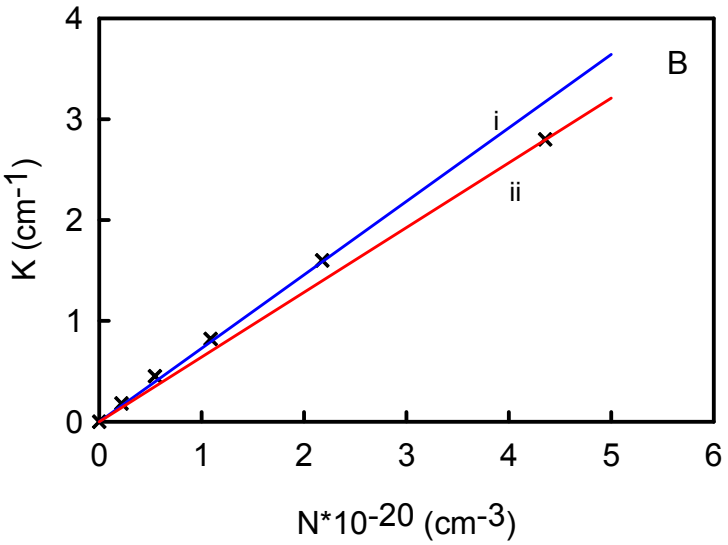

Fig. 6 Dependence of absorption coefficient of Er at 1505 nm as a function of Er concentration (i) Small concentration fit; (ii) fit including 4% concentration of Er.

The RT kinetic of the photoluminescence measured at $^4I_{13/2} \rightarrow {}^4I_{15/2}$ transition was single exponential with lifetime τ=5.6 ms (see Fig. 7) coinciding with the accepted values in modern literature [8]. This lifetime is practically temperature independent and can be considered as radiative lifetime of Er at $^4I_{13/2} \rightarrow {}^4I_{15/2}$ transition.

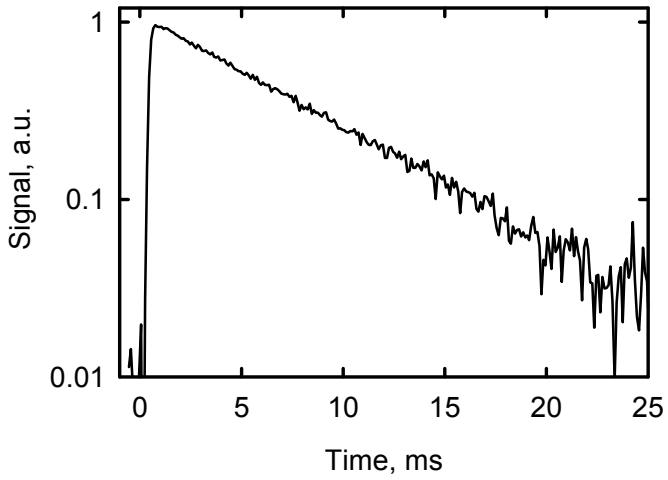

Fig. 7 RT Kinetics of luminescence of 0.25% Er:PWO crystal measured at 1533 nm under 532 nm excitation.

Emission cross section of Er at $^4I_{13/2} \rightarrow {}^4I_{15/2}$ transition at RT were determined using either the reciprocity method (RM) or the Fuchtbauer-Landenburg equation. According to RM method the absorption and emission cross sections are related as:

$$\sigma_{em}(\nu)=\sigma_{ab}(\nu)\frac{Z_l}{Z_u}\exp([E_{zl}-h\nu]/kT), \quad (1)$$

where E_{zl}-is the energy separation between the lowest crystal field components of the upper and lower states, Z_u, Z_l are partition functions that can be obtained using the energy gap (E_i, E_j) from the lowest crystal field level of each manifold, and (g_i, g_j) energy-level degeneracies obtained using the following equations:

$$Z_u=\sum_j g_j \exp(-\Delta E_j/kT) \quad (2)$$

$$Z_l=\sum_i g_i \exp(-\Delta E_i/kT) \quad (3)$$

The Z_l/Z_u factor depends on temperature but does not have any spectral dependence. On the other hand the emission spectra in cross-section units can be obtained with the use of the Fuchtbauer-Landenburg equation:

$$\sigma_{em}(\lambda)=\frac{\lambda^5 I(\lambda)}{8\pi c n^2 \tau_{rad}\int I(\lambda)\lambda d\lambda}, \quad (4)$$

where λ - emission wavelength, $n=2.2$ - refractive index, c - speed of light, τ_{rad} - radiative emission lifetime, and I – intensity of luminescence. In our calculations we assumed that the radiative lifetime is close to τ=5.6 ms.

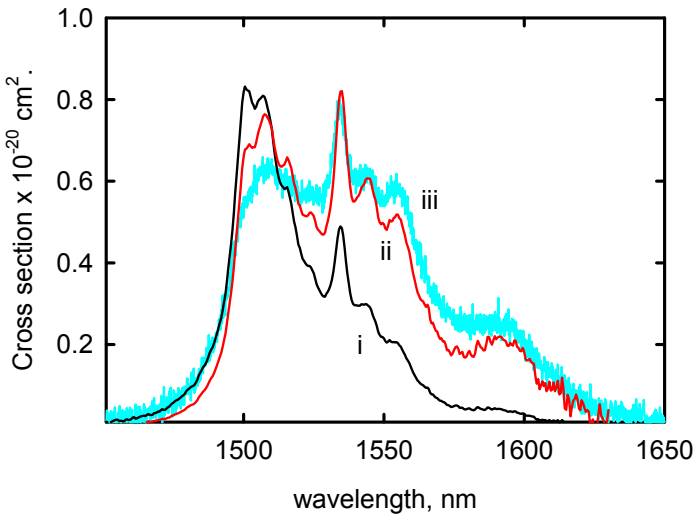

Fig. 8 RT Absorption (i) and emission spectra calculated using reciprocity method (ii) and Fuchtbauer–Landenburg equation (iii).

As one can see from Fig.8, both methods (FL and RT) demonstrate very similar calculated emission cross section profiles. Maximum calculated value of Er:PWO emission cross-section is $\sigma_{em}\approx 0.8\times10^{20}$ cm^2 at 1533 nm.

It was also of great interest to study mid-infrared emission of Er:PWO at $^4I_{11/2}\rightarrow{}^4I_{13/2}$ 2.8 μm transition. Figure 9 demonstrates emission spectrum of 4% Er:PWO at $^4I_{11/2}\rightarrow{}^4I_{13/2}$ transition measured at room temperature. As one can see the mid-infrared luminescence band is broadened, features FWHM of ~ 150 nm and is promising for lasing tunable over 2670-2870 nm spectral range.

5 Conclusions

In conclusion, the absorption and luminescence properties of Er:PWO crystals in the visible and near infrared spectral ranges were studied at room and low temperatures. The maximum absorption cross section was estimated to be $\sigma=8.0\text{x}10^{-21}$ cm^2 at 1505 nm and E||z polarization of incident light. The measured luminescence lifetime at $^4I_{13/2}\rightarrow{}^4I_{15/2}$ transition was 5.6 ms. The maximum emission cross section was estimated to be $\sigma=8.0\text{x}10^{-21}$ cm^2 at 1533 nm.

Luminescence spectrum of Er:PWO at ${}^4I_{11/2} \rightarrow {}^4I_{13/2}$ transition centered at 2730 nm is broadened, features FWHM of ~ 150 nm and is promising for lasing tunable over 2670-2870 nm spectral range.

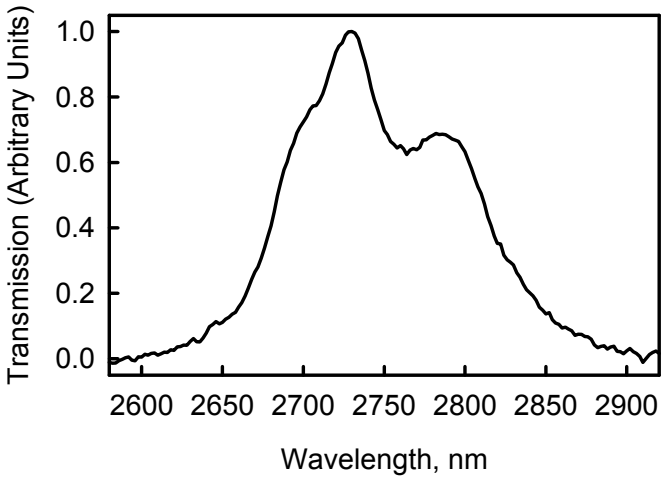

Fig. 9 Luminescence spectrum of 4% Er:PWO at ${}^4I_{11/2} \rightarrow {}^4I_{13/2}$ transition measured at room temperature.

6 Acknowledgement

We acknowledge support from the National Aeronautics and Space Administration (NASA)-Alabama Space Grant Consortium - Research Experiences for Undergraduates (REU) award to UAB. This material is also partially based upon work supported by NSF grant EPS-0814103. We also acknowledge North Crystals Co. for providing the crystals used in this study.

7 References

1 "Some Aspects of the Luminescence of Solids", F.A. Kroger, Elsevier, Amsterdam, 1948.

2 Compact Muon Solenoid Technical Proposal, CERN/LHCC94-38, LHCClPl, 1994.

3 A.A. Kaminskii, H.J. Eichler, K. Ueda, N.V. Klassen, B.S. Redkin, L.E. Li, J. Findeisen, D. Jaque, J. Garcia-Sole, J. Fernandez, R. Balda, "Properties of Nd^{3+}-Doped and Undoped Tetragonal $PbWO_4$, $NaY(WO_4)_2$, $CaWO_4$, and Undoped Monoclinic $ZnWO_4$ and $CdWO_4$ as Laser-Active and Stimulated Raman Scattering-Active Crystals", Appl.Opt. 38, 4533-4547 (1999).

4 A.A. Kaminskii, C.L. Mccray, H.R. Lee, S.W. Lee, D.A. Temple, T.H. Chyba, W.D. Marsh, J.C. Barnes, A.N. Annankov, V.D. Legun, H.J. Eichler, G.M.A. Gad, K. Ueda, "High efficiency nanosecond Raman lasers based on tetragonal PbWO crystals", Opt.Commun. 183, 277-287 (2000).

5 T.T. Basiev, A.A. Sobol, Yu.K. Voronko, P.G. Zverev, "Spontaneous Raman spectroscopy of tungstate and molybdate crystals for Raman lasers", Opt. Mater. 15, 205-216 (2000).

6 W. Chen, Y. Inagawa, T. Omatsu, M. Tateda, N. Takeuchi, Y. Usuki, "Diode-pumped, self-stimulating, passively Q-switched Nd^{3+}:$PbWO_4$ Raman laser", Opt. Commun. 194, 401-407 (2001).

7 S.A. Payne, L.L. Chase, L.K. Smith, W.L. Kway, W. Krupke, "Infrared Cross-Section Measurements for Crystals Doped with Er^{3+}, Tm^{3+}, and Ho^{3+}", IEEE J. Quantum Electron. 28, 2619-2630 (1992).

8 Y. Huang, H.J. Seo, W. Zhu, Y. Yang, "Room-temperature 1.53μm emission in Er^{3+}-doped $PbWO_4$ single crystals", Phys. Stat. Sol. 202, 462-468 (2005).